Journal of Power Sources 249 (2014) 397–404

Contents lists available at ScienceDirect

Journal of Power Sources

journal homepage: www.elsevier.com/locate/jpowsour

Novel polymer electrolytes based on cationic polyurethane with different alkyl chain length

Libin Liu*, Xiwen Wu, Tianduo Li

Shandong Provincial Key Laboratory of Fine Chemicals, Key Laboratory of Fine Chemicals in Universities of Shandong, Qilu University of Technology, Jinan 250353, PR China

HIGHLIGHTS

- A series of comb-like cationic polyurethane electrolytes were synthesized.
- Alkyl quaternary ammonium salts are recognized as inherent plasticizers.
- Ionic conductivity is the charge migration between coordination sites and aggregates.
- The plasticizing effects of longer alkyl chain electrolytes are more effective.
- The systems behave like a liquid while preserving the dimensional stability.

ARTICLE INFO

Article history:
Received 13 August 2013
Received in revised form
18 October 2013
Accepted 24 October 2013
Available online 6 November 2013

Keywords:
Cationic polyurethane
Solid polymer electrolyte
Alkyl quaternary ammonium salts
Comb-like

ABSTRACT

A series of comb-like cationic polyurethanes (PUs) were synthesized by quaternizing different bromoalkane (C_2H_5Br, $C_8H_{17}Br$, and $C_{14}H_{29}Br$) with polyurethane. Solid polymer electrolytes were prepared by complexes cationic PUs with different content of $LiClO_4$. All the solid polymer electrolytes had sufficient thermal stability as confirmed by TGA and exhibited a single-phase behavior evidenced by DSC results. For these electrolytes, FT-IR spectra indicated the formation of polymer–ion complexes. The ac impedance spectra show that the conductivity of the electrolytes follow the Arrhenius behavior, and ionic conductivity is associated with both the charge migration of ions between coordination sites and transmission between aggregates, as confirmed by FT-IR and SEM. Alkyl quaternary ammonium salts in the polymer backbone are recognized as inherent plasticizers, which make the electrolytes exhibit liquid-like behavior. The plasticizing effect of PU-C_8 and PU-C_{14} electrolytes are more effective than that of PU-C_2 electrolyte. Maximum ionic conductivity at room temperature for PU-C_8 electrolytes containing 50 wt% $LiClO_4$ reached 1.1×10^{-4} S cm^{-1}. This work provides a new research clue that alkyl quaternary ammonium salts could be used as inherent plasticizers and hence make the system behave like a liquid with high ionic conductivity, while preserving the dimensional stability of the solids.

1. Introduction

Recently, solid polymer electrolytes (SPEs) have attracted worldwide attention and been investigated widely in lithium-ion batteries [1,2], chemical sensors, data storage and electrochemical devices [3]. Lithium-ion doped SPEs offer many advantages such as ease of manufacturing, immunity from leakage, suppression of lithium dendrite formation, elimination of volatile organic liquids and mechanical flexibility. However, the main problem in achieving the expected applications is their low ionic conductivity.

Thermoplastic polyurethane has two-phase microstructure: the soft segments and the hard segments and have been largely employed as matrix materials for polymer electrolytes [4–13]. The hard segments are interconnected throughout the soft phase parts, and act as reinforcing fillers and hence contribute to the mechanical strength of the polymer electrolytes. While the low glass transition temperature (T_g) and hence higher segmental motion of their soft segments dissolve alkali metal without formation of ionic cluster and offer the whole system with good ionic conductivity. Because of the solvation power and complexing ability of poly(ethylene oxide) (PEO) to alkali metal ion, many studies on SPEs have dealt with polyurethane consisting of polyether-like structure with lithium salts. The transport mechanism within SPEs based on PEO and salts has been recognized that the ionic conductivity of PEO-based

* Corresponding author. Tel./fax: +86 531 89631208.
E-mail addresses: lleebin@hotmail.com, lbliu@qlu.edu.cn (L. Liu).

0378-7753/$ – see front matter © 2013 Elsevier B.V. All rights reserved.
http://dx.doi.org/10.1016/j.jpowsour.2013.10.116

electrolytes is facilitated in the amorphous phase of PEO [14]. Various approaches have been devoted in tailing a polymer structure having a highly flexible backbone and a larger proportion of the amorphous phase. For instance, random copolymers [15,16], block copolymers [17,20], comb polymers [18] and crosslinked networks [19] have been explored and their electric properties have been investigated. Despite considerable interest in and effort devoted to SPEs, studies on the conductivity mechanism of the SPEs based on cationic polyurethane are still relatively limited.

Herein, we demonstrate for the first time the study on the properties of solid polymer electrolytes based on the cationic polyurethane. By inducing different bromoalkane (C_2H_5Br, $C_8H_{17}Br$, and $C_{14}H_{29}Br$) into polyurethanes, comb-like polymers with different alkyl chain length were synthesized. Solid polymer electrolytes were prepared by complexing the polymers with $LiClO_4$. The aim of this study is to identify the influence of the polyurethane backbone (different alkyl chain length) and the effect of the ionic salt concentration on the SPEs based on different bromoalkane quaternized polyurethane by conducting FT-IR study along with DSC, SEM and alternating current (ac) impedance measurements.

2. Experimental section

2.1. Materials

Poly(ethylene glycol) (PEG; molecular weight 600; Aladdin Industrial Inc.) was dehydrated under reduced pressure at 90 °C for 2 h before using. 4,4′-Methylenebis(phenyl isocyanate) (Aladdin), *N*,*N*-Methyldiethanolamine (MDEA, Aladdin) and $LiClO_4$ (Aladdin) were used as received. *N*,*N*-Dimethylforamide (DMF, Sinopharm Chemical Reagent Co., Ltd) was distilled fractionally over CaH_2 under reduced pressure and stored over 4 Å molecular sieves. All the other reagents and chemicals were used without further purification.

2.2. Synthesis of cationic PU

All the polyurethanes were synthesized by a two-step addition process in which the prepolymer was made by reaction of excess of MDI with MDEA and then the end NCO groups were reacted with chain extender of PEG (Scheme 1). The reaction was detected by *in-situ* FTIR and the completion of prepolymer formation was confirmed by half of the intensity of NCO group. The molar ratio of MDI, MDEA, and PEG was 2:1:1. The structure of the synthesized PU is shown in Scheme 1. Appropriate amount of bromoalkane (C_2H_5Br, $C_8H_{17}Br$ and $C_{14}H_{29}Br$) and PU were reacted in DMF solution at 85 °C for 30–36 h. The molar ratio of bromoalkane and DMEA was kept at 3:1. After the solution was cooled to ambient temperature, it was dropped into water. The polymer was filtered and washed with hexane to remove excessive bromoalkane, finally dried in a vacuum desiccator. ^{1}H NMR spectra were recorded on a Bruker AVANCE II 400 spectrometer using tetramethylsilane (TMS; $\delta = 0$ ppm) as the internal standard. Gel permeation chromatography (GPC) was used to determine the molecular weights of polymers. GPC analysis was performed on a Wyatt DAWN HELEOS system (50 Mw GaAs, $\lambda = 650$ nm). Polystyrene standards were used as calibration standards for GPC. The synthesized cationic polyurethanes are abbreviated to PU-C_2, PU-C_8 and PU-C_{14}, respectively.

PU-C_2 was obtained as light yellow sticky-solid. Mw = 21.35 K, Mw/Mn = 1.57 (GPC, polystyrene calibration). ^{1}H NMR (d_6-DMSO) δ (ppm): 0.8 (−C*H*$_3$), 1.1–1.2 (−C*H*$_2$−), 3.1–3.2 (−OC*H*$_2$−), 3.3–3.5 (−OC*H*$_2$−), 7.0–7.1 (Ar*H*), 7.2–7.4 (Ar*H*), 8.5–8.6 (−N*H*−), 9.5–9.7 (−N*H*−).

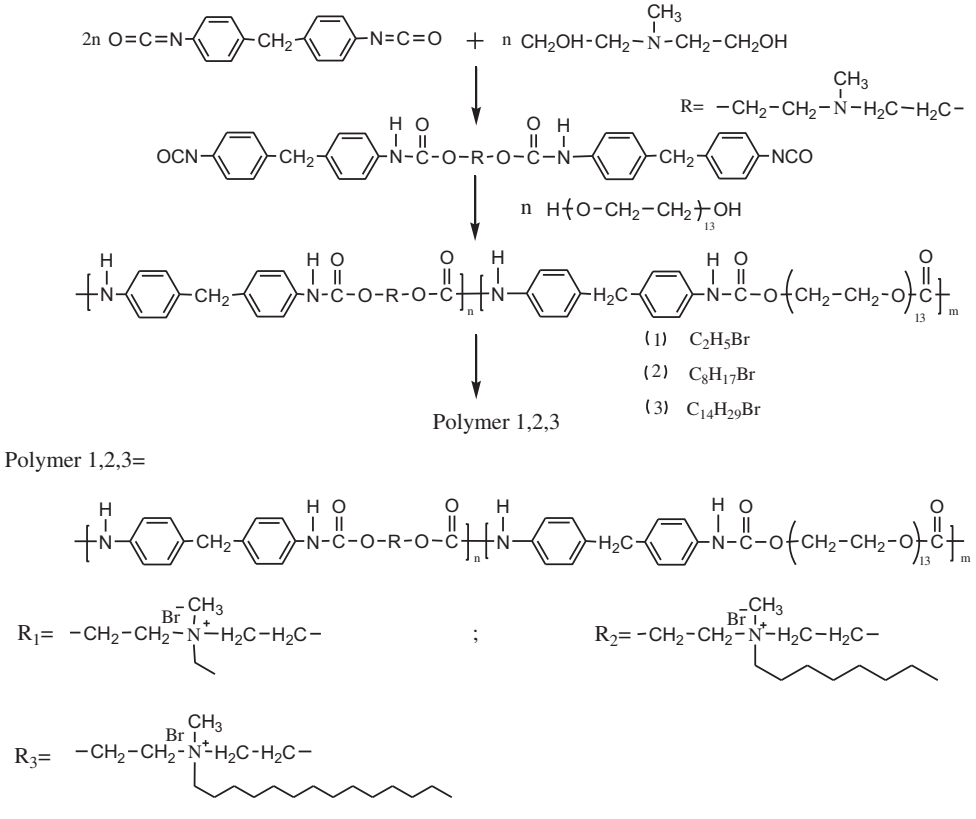

Scheme 1. Schematic representation of synthesis of cationic PUs.

PU-C_8 was obtained as light yellow sticky-solid. Mw = 22.87 K, Mw/Mn = 1.48 (GPC, polystyrene calibration). ^{1}H NMR (d_6-DMSO) δ (ppm): 0.9 (−CH_3), 1.2–1.5 (−CH_2−), 3.1–3.3 (−OCH_2−), 3.4–3.6 (−OCH_2−), 7.0–7.1 (ArH), 7.1–7.3 (ArH), 8.4–8.5 (−NH−), 9.6–9.7 (−NH−).

PU-C_{14} was obtained as light yellow solid. Mw = 24.36 K, Mw/Mn = 1.52 (GPC, polystyrene calibration). ^{1}H NMR (d_6-DMSO) δ (ppm): 0.8 (-CH_3), 1.2–1.6 (−CH_2−), 3.1–3.3 (−OCH_2−), 3.3–3.5 (−OCH_2−), 7.0–7.1 (ArH), 7.2–7.3 (ArH), 8.5–8.6 (−NH−), 9.7–9.8 (−NH−).

2.3. Preparation of polymer electrolytes

Solid polymer electrolytes (SPEs) were prepared by mixing various amounts of $LiClO_4$ and a cationic PU solution in DMF, and continuously stirred at 60 °C for 24 h. Finally DMF was removed under reduced pressure and dried at 80 °C for 12 h in a vacuum desiccator to achieve the desired SPEs.

2.4. Differential scanning calorimetry

The DSC experiments were carried out using a DSC 2000 differential scanning calorimenter (TA Instruments, USA) over the temperature range −80 °C to 120 °C. Temperature was calibrated using an indium standard. The sample films were cut and weighed from 8 to 10 mg. Samples were first heated from 25 °C to 120 °C and cooled to −80 °C at 15 °C min^{-1}, and then reheated to 120 °C at 15 °C min^{-1}. Data reported herein were taken from the second heating cycle and were analyzed using TA universal analysis software.

2.5. Thermogravimetric analysis

The thermal stability of the films was monitored using thermogravimetric analysis (SDT Q600). The TGA measurements were carried out under dry nitrogen atmosphere at a heating rate of 10 °C min^{-1} from 30 to 700 °C.

2.6. Fourier transform infra-red spectroscopy

FT-IR spectra were taken at ambient temperature using an IR Prestige-21 spectrometer (Bruker) operating at a resolution of 0.5 cm^{-1}. All IR spectra were obtained within the range 4000–400 cm^{-1} by casting the samples on the KBr disk.

2.7. X-ray diffraction

X-ray diffraction patterns of all the solid polymer electrolytes were obtained in a D8-ADVANCE diffractometer using Cu Ka radiation. Sweeps from 3° to 70° at 0.03° s^{-1} were performed.

2.8. Conductivity measurements

Ionic conductivity measurements with alternation current were conducted on a CHI660D within a frequency range from 100 KHz to 0.1 Hz under an oscillation potential of 10 mV. The electrolyte film was sandwiched between stainless steel blocking electrodes (diameter: 0.66 cm). The specimen thickness varied from 2.1 to 2.4 mm; the impedance response was gauged over the range from 20 °C to 80 °C. Complex impedance plots (semi-circles) were computed from the raw experimental data. The intersection in the imaginary impedance at low frequency with the real impedance axis corresponds to the ionic conductance of the samples and hence the conductivity values (σ) were calculated from the bulk resistance according to the equation [20].

$$\sigma = L/AR_b \quad (1)$$

where σ is the conductivity, L is the thickness of the electrolyte film, A is the section area of the stainless steel electrode, and R_b is the bulk resistance.

3. Results and discussion

3.1. Influence of salt on bulk properties

The thermal stability study of the solid polymer electrolytes is very important for their applications in technological devices. As can been seen from Fig. 1a, the degradation temperature of the cationic PU (PU-C_2, PU-C_8, PU-C_{14}) was slightly decreased compared to that of pure PU. The thermal degradation of PU-C_2 occurs in two stages. The first stage is mainly related to the breaking of rigid segments, and involves the dissociation of urethane in the original isocyanate and chain extender, that then form primary amine, alkenes and carbon dioxide. During the second stage, in which the flexible segments are involved, both depolycondensation and polyol degradation mechanisms take place [5,21]. For PU-C_8 and PU-C_{14}, another stage occurs, which should be related to degradation of the alkyl vertex groups in the rigid segments of cationic PU [22].

The introduction of salt promotes polymer/salt complex degradation. The degradation temperature at a 5% weight loss ($T_{d,5\%}$) of the samples obtained from the TGA measurements are summarized in Table 1. $T_{d,5\%}$ values decreased with an increase in the $LiClO_4$ content. This behavior may be explained by the weakness of the C–O bond, caused by the electronic density decreasing the O–Li^+ interaction [9] (The interaction of salts with cationic PU is discussed in the following FT-IR parts). $T_{d,5\%}$ values of the cationic PU/salt complexes were observed above 155 °C, indicating that the complexes had sufficient thermal stability for use as the polymer electrolyte matrix in lithium batteries even at the elevated temperature.

The thermal properties of the polymers were examined using differential scanning calorimetry (DSC). Fig. 2 shows the DSC thermograms of cationic PU-C_2 and PU-C_8 with and without $LiClO_4$. For pure PU-C_2 and PU-C_8, the inflections of DSC curves were shown a broad glass transition temperature centered at 31.4 °C and 41.1 °C, respectively, which in the range of 20–100 °C can be assigned to be the T_g of hard segment of urethane group from MDI like the reported T_g for urethane [23]. The thermal transitions associated with soft segments were not prominent in DSC thermograms due to high hard segments contents (Hard segments: 54.8 wt%, 57.5 wt%, 59.9 wt% for PU-C_2, PU-C_8 and PU-C_{14}, respectively) of the cationic PU used in this study. Upon adding $LiClO_4$, the glass transition temperatures of the cationic PU decreased with increasing lithium contents (Fig. 2, Table 1), indicating that the lithium ions interact with the hard segments. This effect decreases the extend of the H-bond between the hard segments and soft segments and thus decreases the T_g. Similar trends were observed for PU and PU-C_{14} electrolyte (Fig. S1 in supporting information). These T_g trends are also corroborated by the ionic conductivity measurements shown below.

The XRD data revealed that the three kinds of cationic PU are all amorphous system structures, as shown by the presence of broader peaks in Fig. 3. The addition of salts induce a significant amorphous structure in the polymer matrix, as evident from the less intense and broad peak obtained at $2\theta = 21.5°$. Similar changes were also observed in PU-C_2 and PU-C_{14} electrolytes (Fig. S2 in the supporting information). These results are consistent with the DSC measurements which show a single T_g in all the polymer–salt complexes. In previous studies, it has been pointed out that the ionic conductivity

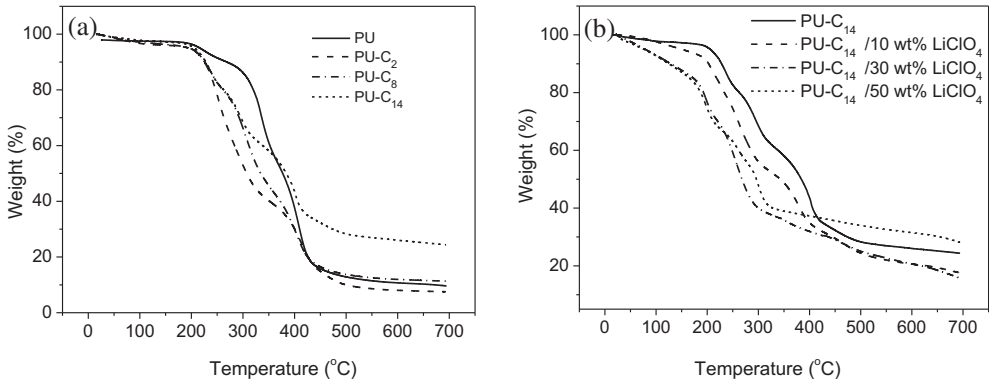

Fig. 1. Thermogravimetry curves of PU and cationic PU (a) and PU-C_{14} with different amount of $LiClO_4$ (b).

Table 1
Thermal properties of the PU and cationic PU with different $LiClO_4$ contents.

$LiClO_4$ content (wt%)	PU		PU-C_2		PU-C_8		PU-C_{14}	
	T_g (°C)	$T_{d,5\%}$ (°C)	T_g (°C)	$T_{d,5\%}$ (°C)	T_g (°C)	$T_{d,5\%}$ (°C)	T_g (°C)	$T_{d,5\%}$ (°C)
0	12.5	241	31.4	201	41.1	205	35.3	211
10	3.6	238	1.5	198	21.5	200	18.4	203
20	−7.8	208	−12.8	193	−1.7	195	−2.1	188
30	−17.8	205	−18.1	187	−19.5	188	−24.1	160
40	−26.6	187	−32.2	183	–	178	–	158
50		148	–	176	–	173	–	155

$T_{d,5\%}$, is the decomposition temperature and defined as 5 wt% loss.

takes place in the amorphous regions of the polymer system and that crystalline domains act as potential barriers [24]. Therefore, these results demonstrate that the polymer–salt complexes are amorphous and they are not homogeneous; however, they could have a promising high ionic conductivity.

3.2. Polymer–salt interaction of cationic PU electrolytes

FT-IR spectroscopy has been conducted at ambient temperature to examine the effects of alkali metal salt concentration on the interaction of Li^+ with groups in the cationic PU. In Fig. 4a, the NH stretching vibration exhibits a strong absorption peak centered at around 3200–3300 cm^{-1} arising from the hydrogen bonding between NH and carbonyl groups, whereas the free NH stretching vibration appears at ca. 3500–3520 cm^{-1}. Note that there appears another obvious peak at 3170 cm^{-1}, which should be the NH groups that hydrogen bonded to ether group [25]. Upon adding $LiClO_4$, the free NH stretching vibration peak is enhanced due to the interaction between the Li^+ cation and the lone pair of electrons on the nitrogen atom (Scheme 2a) [26]. In addition, with increasing $LiClO_4$ content, the band of NH group hydrogen bonded to ether group disappeared and the band of hydrogen bonding between NH and carbonyls was shifted to high wavenumbers and centered at 3375 cm^{-1}. Because the band position is related to the strength of the H-bonded NH bond, then the shift to higher frequency with increasing salt concentration indicated an increase in the bond strength of the N–H bond. This indicates that Li^+ ions preferentially coordinate to the electron-rich oxygens (carbonyls and ether groups) as shown in Scheme 2b and c [6,27].

In Fig. 4b, the pristine PU-C_8 exhibits several characteristic bands, including 1727 cm^{-1} (free C=O of urethane), 1709 cm^{-1} (hydrogen-bonded C=O of urethane) and 1694 cm^{-1} (free amide I), revealing that fraction of these urethane are hydrogen bonded [28]. Upon adding $LiClO_4$ to the PU-C_8 polymer, the intensities of the urethane C=O group centered at 1717 cm^{-1} with the disappearance of the free amide I band (1694 cm^{-1}). Additionally, an ordered "complexed" C=O bands appeared at 1664 cm^{-1} and increased with increasing $LiClO_4$ concentration. This may be attributed to the coordination of electron deficient Li^+ ions with carbonyl oxygen atoms, which weakens the C=O bond by sharing the electron density of the carbonyl oxygen atoms (Scheme 2b).

Fig. 4c shows the changes in the position of the C–O–C symmetric and asymmetric stretching at 1143, 1112 and 1088 cm^{-1} for pristine PU-C_8 [29]. Upon adding $LiClO_4$, the triple bands become broad and merge into a single peak with the absorption maximum at 1101 cm^{-1}. This may be due to the interaction of Li^+ ions with the ether oxygen leading to a decrease in the electron density of this oxygen and in its ability to form H-bonds (Scheme 2c).

One of the important properties that can be estimated from FT-IR is the ionic association. The characteristic $\nu(ClO_4^-)$ mode of $LiClO_4$ is particularly sensitive in changing the ion–ion interactions in the electrolyte systems. As shown in Fig. 4d, the band centered at 625 cm^{-1} has been assigned to the vibration of the "free" ClO_4^- anion, which does not interact directly with the lithium cations, whereas the shoulder centered at 635 cm^{-1} is due to the vibration

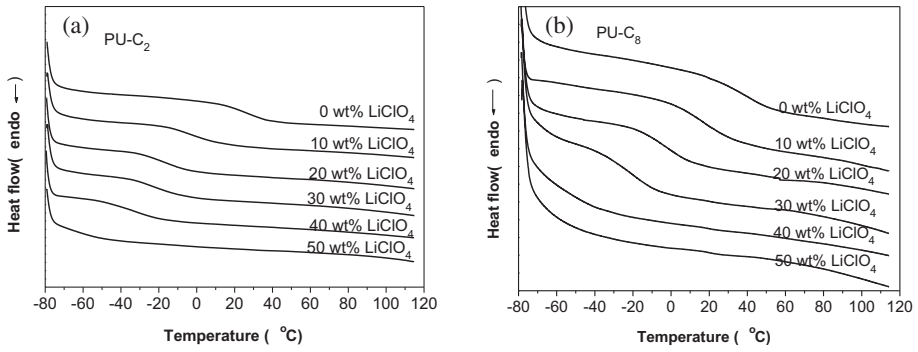

Fig. 2. DSC thermograms of cationic PU-C_2 (a) and PU-C_8 (b) with various $LiClO_4$ content.

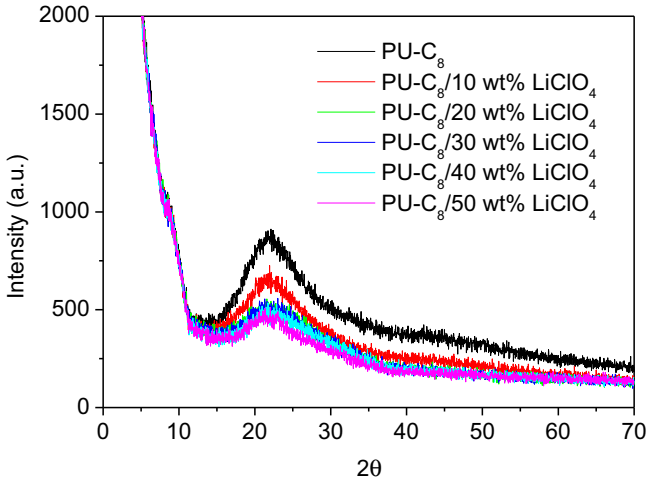

Fig. 3. XRD pattern of neat PU-C_8 and PU-C_8/$LiClO_4$ complexes.

of the Li^+ ClO_4^- contact–ion pairs as the $LiClO_4$ concentration increased [30]. In addition, another peak appeared at 678 cm^{-1} when the concentration of $LiClO_4$ increased to 30 wt%. This may be due to the vibration of the Li^+Br^- contact–ion pairs. At high $LiClO_4$ concentration, the anion (Br^-) in the alkyl quaternary ammonium salts may exchange with ClO_4^-.

From the FTIR analysis, it could be found that Li^+ ion could possibly coordinate in different domains (see Scheme 2), namely hard and soft domains in cationic PU polymer matrix. For PU-C_2 and PU-C_{14} electrolytes, introduction of Li salt results in the similar interaction with the groups of polymer matrix (Figs. S3 and S4 in the supporting information). The alkyl chains in the cationic PU do not affect the interaction of Li^+ with groups in the cationic PU,

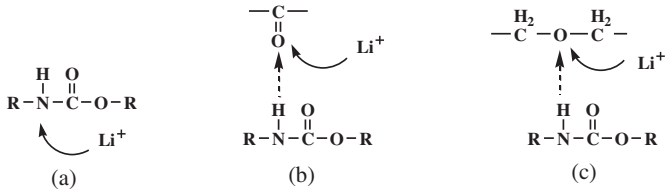

Scheme 2. Schematics for the suggested coordination of lithium salt with groups of cationic PU.

compared to that in PU (Fig. S5 in the supporting information). In this case, the fraction of the hydrogen-bonded carbonyls is defined by a hard–hard segment hydrogen bond (NH···O=C bond), which was employed to evaluate the extent of phase separation. On the other hand, the fraction of the hydrogen bonded ether oxygens (NH···O bond) represents the extent of phase mixing between hard and soft segments. Combined with DSC analysis which shows a single T_g, with addition of $LiClO_4$, the hard segments and soft segments are miscible into a single phase, favorable for the ion conductivity.

3.3. Ionic conductivity of cationic PU electrolytes

The ionic conductivities of cationic PUs were investigated as a function of temperature and lithium salt concentration as show in Fig. 5. For PU and all bromoalkane quaternized PU, the plot of the ionic conductivity against the reciprocal absolute temperature is linear, indicating that the conductivity of the polymer electrolyte obeys Arrhenius law. The Arrhenius relationship indicates that the charge carriers are decoupled from the segmental motion of polymer chain, and the conductive environment of Li^+ ions in the SPEs is liquid-like, remaining unchanged in the measured temperature range. The Arrhenius equation can be described as

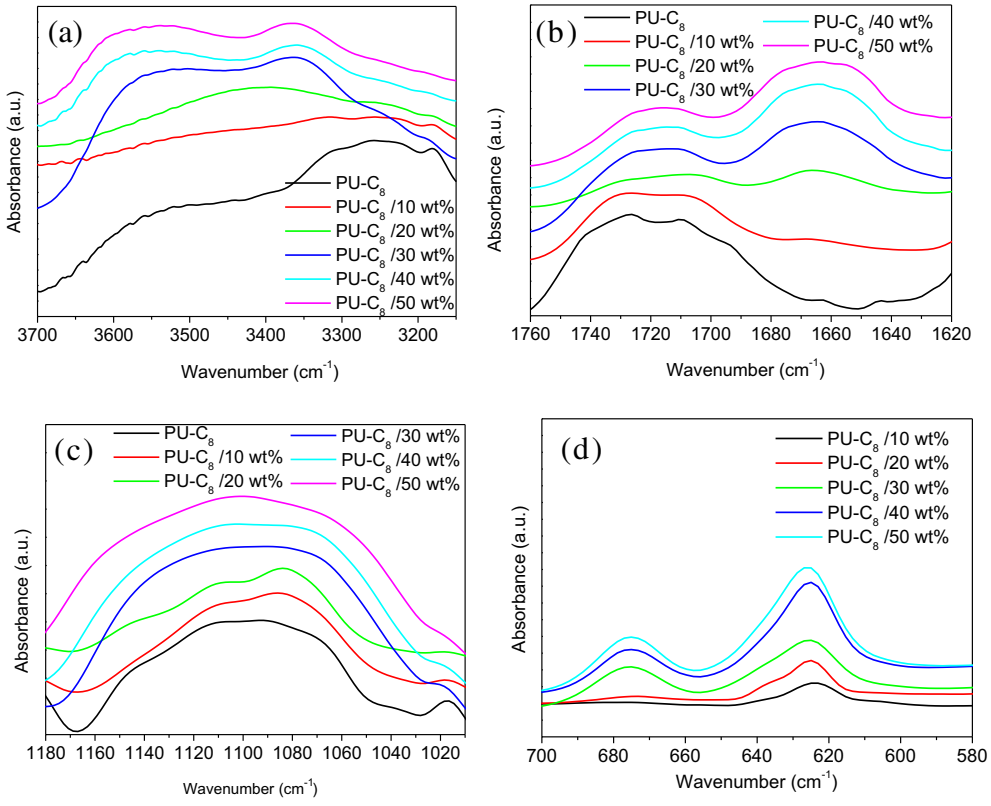

Fig. 4. FT-IR spectra for PU-C_8/$LiClO_4$ complexes in the wavenumber rangers 3700–3100 cm^{-1} (a), 1760–1620 cm^{-1} (b), 1180–1000 cm^{-1} (c), 700–580 cm^{-1} (d), respectively.

$$\sigma = \sigma_0 \exp(-E_a/kT) \quad (2)$$

where σ is the ionic conductivity, σ_0 is the pre-exponential factor, E_a is the activation energy and k is the Boltzmann's constant. As the conductivity plot fits well with the Arrhenius equation in the temperature range of 20–80 °C (Fig. 5), the activation energies (E_a) are calculated from this temperature range and listed in Table 2.

For PU, the ionic conductivity increased rapidly with salt concentration, reached a maximum at 40 wt% $LiClO_4$ content, and thereafter decreased (Fig. 5a). This may be due to the interplay between opposing effects. On one side, the number of charge carriers increases with increasing amount of salt. On the other side, the presence of salt increases the glass transition temperature (as a result of the interaction of Li^+ ions with the ether oxygen) and leads to the decrease of free volume, although the T_g of soft segments is not detected in our case due to high hard segments contents (51.1 wt%). Additionally, at such salt concentrations a considerable amount of salt remains as ion-pairs, that do not contribute to the conductivity of the electrolytes. This was confirmed by the characteristic $\nu(ClO_4^-)$ mode of $LiClO_4$ in changing the ion–ion interactions in the electrolyte systems (Fig. S5 in the supporting information). In addition, $LiClO_4$ crystal is appeared when the concentration of $LiClO_4$ increased to 50 wt%, whereas the PU electrolytes with 40 wt% $LiClO_4$ content revealed smooth surface (Fig. S6 in the supporting information).

For all cationic PU electrolytes, the E_a values decreased with increasing the salt concentrations, the low E_a values indeed suggest the presence of significant ionic mobility in the electrolytes in this temperature range. The ion transport is decoupled from the polymer chains and thermally activated ionic hopping produces higher conductivities for these hybrid electrolytes in the temperature range.

Comparing Fig. 5b with c and d, it was observed that as the salt concentration increased, the log σ vs. T^{-1} curves of PU-C_8/$LiClO_4$ electrolytes and that of PU-C_{14}/$LiClO_4$ electrolytes shifted up with much larger interval value than that of PU-C_2 electrolytes with $LiClO_4$. This indicated that the ionic conductivity of PU-C_2/$LiClO_4$ electrolytes was much less sensitive to the lithium salt concentration than PU-C_8/$LiClO_4$ electrolytes and PU-C_{14}/$LiClO_4$ electrolytes. This difference was associated with the microstructure of cationic PU, which may be ascribed to the additional free volume generated by the long and random orientation of the alkyl substitutes in the polymer. A maximum ion conductivity of 1.1×10^{-4} S cm^{-1} at room temperature was found for PU-C_8 with 50 wt% $LiClO_4$ content.

Table 2
The ionic conductivity at room temperature σ and activation energies E_a of cationic PU/$LiClO_4$ electrolytes.

	$LiClO_4$ (wt%)	Conductivity at 300 K (S/cm)	E_a (eV)
PU	10	1.52×10^{-8}	0.47
	20	2.12×10^{-8}	0.47
	30	4.85×10^{-7}	0.37
	40	1.33×10^{-5}	0.30
	50	4.45×10^{-6}	0.34
PU-C_2	10	2.03×10^{-7}	0.43
	20	4.56×10^{-7}	0.40
	30	1.93×10^{-6}	0.33
	40	5.19×10^{-6}	0.31
	50	8.79×10^{-6}	0.28
PU-C_8	10	1.94×10^{-8}	0.44
	20	1.59×10^{-7}	0.36
	30	1.43×10^{-6}	0.32
	40	4.68×10^{-5}	0.25
	50	1.07×10^{-4}	0.24
PU-C_{14}	10	1.44×10^{-8}	0.47
	20	1.83×10^{-7}	0.37
	30	2.18×10^{-6}	0.32
	40	2.15×10^{-5}	0.21
	50	7.99×10^{-5}	0.20

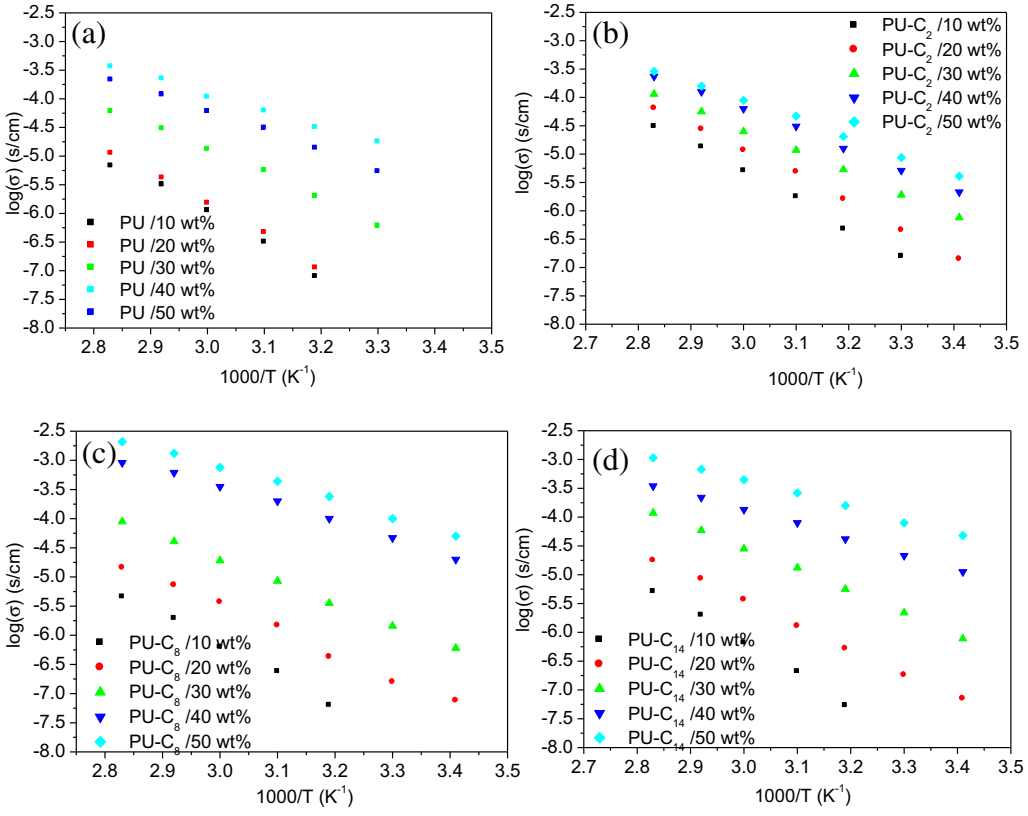

Fig. 5. Ionic conductivities of SPEs based on (a) PU, (b) PU-C_2, (c) PU-C_8, (d) PU-C_{14} with different $LiClO_4$ concentration.

It should be noted that the conductivity curves of cationic PU did not show any signs of the melting of the hydrocarbon side chains, similar to the results detected by DSC showing only one T_g. The same behavior was observed for polymer electrolytes based on comb polymers having hydrocarbon chains attached to the ends of the PEO side chains [31]. The present finding indicated that the alkyl chains attached to the polymer backbone are disordered distributed in the polymer matrix. Thus, it seemed like the hydrocarbon domains remained intact, or that the degree of crystallinity of the hydrocarbon side chains was too low to influence the chain mobility in a significant way.

3.4. Morphology of cationic PU electrolytes

Since ionic conductivity is associated with interactions of molecular dipoles and mobility of charges, it is therefore strongly dependent on the spatial distribution of ionic sites and hence on the morphology of a specific sample. Low revolution SEM images show a smooth surface for all cationic PU/$LiClO_4$ complexes. Close inspection of morphological behavior explores the samples ionic conductivity; high revolution images of electrolyte film are shown in Fig. 6. For PU-C_2 electrolyte, sphere-like morphologies with the size of about 100 nm were observed in the full coverage. For PU-C_8, the surface of the electrolytes shows irregular aggregates with numbers of pores. More loosely packed grains were observed in PU-C_{14}/$LiClO_4$ electrolyte films. No scan images were showed any separated phase for the cationic PU/$LiClO_4$ complexes, which confirms the complete dissolution of the salt in the medium. Recently, Ng et al. [32] investigated a urethane cross-linked PEG polymer doped with $LiClO_4$ and $LiCF_3SO_3$ and indicated a shift in the mechanism of ion mobility, where Li ions are transmitted between aggregates, and hence is less influenced by the segmental motion of the polymer chains. In our case, all the cationic PU revealed the presence of the aggregates in which aggregates associate with weak van der Waals forces rather than strong coulombic interactions and their facile mobility would account for the low activation energies. The ionic conductivity in these systems may occur primarily in the amorphous regions and is associated with both the charge migration of ions between coordination sites and transmission of ions between aggregates.

The temperature dependence of conductivity in SPEs may exhibit one of the five behaviors: (a) Vogel–Tamman–Fulcher (VTF) behavior throughout the available temperature range; (b) Arrhenius behavior at low temperatures and VTF behavior at high temperatures; (c) Arrhenius behavior throughout the temperature range, but with two different activation energies; (d) VTF behavior for temperatures slightly greater than the glass transition temperature T_g, but Arrhenius behavior at higher temperature; and (e) the behavior which is very unlike either Arrhenius or VTF at all temperatures [33]. In our case, the conductivity of all the polymer electrolytes fit well with Arrhenius law in the measured temperature range. At low concentrations of $LiClO_4$, the lithium salt is completely dissociated, and the number of mobile ions increases with lithium salt concentration. When the salt concentration reaches 30 wt%, the FT-IR spectra are almost unchanged, indicating that the salt doping level for cationic PU has been saturated (Fig. 4). As the concentration of external doping salt is further increased, the concentration of lithium ions is naturally increased. The dissociated ions Li^+ and ClO_4^- can form ion-pairs, reducing the ionic conductivity. However, this phenomenon is not observed in our systems. The ac impedance spectra show that the conductivities of the cationic PU electrolytes are increased linearly with increasing the $LiClO_4$ concentration, which are different from that of the thermoplastic polyurethane-based polymer electrolytes showing that the ion conductivity reaches a maximum and decreases as the salt concentration further increases reported before [27,34]. In our systems, the alkyl chains attached to the polyurethane backbone to form comb-like polymers. Alkyl quaternary ammonium salts may serve as inherent plasticizers and provide a liquid-like environment within the polymer matrix, similar to the liquid electrolyte systems [35] and gelled polymer electrolyte systems [36] in which the Arrhenius behavior is more commonly found. When the concentration of the $LiClO_4$ reached 40 wt% and 50 wt%, no apparent T_g was detected by DSC (Fig. 2, Table 1) and the activation energies (E_a) are very similar for PU-C_8 and PU-C_{14} electrolytes (smaller than 0.01 ev) (Table 2). This phenomenon supported the hypothesis that alkyl quaternary ammonium salts act as inherent plasticizers and the electrolytes are liquid-like matrixes. In addition, the ac impedance spectra suggest that the plasticizing effect of PU-C_8 and PU-C_{14} electrolytes are more effective than that of PU-C_2 electrolyte due to the longer alkyl chain length.

It should be mentioned that the plasticizers used in polymer electrolytes, such as propylene carbonate [37], ethylene carbonate [38], and dimethyl carbonate [39], provide a liquid-like environment within the polymer matrix, but destroy the dimensional stability of the solids. In our case the molecular inherent plasticizers are different from the external added plasticizer, which make the system not only behave like a liquid with high ionic conductivity but also preserve the dimensional stability and thermal stability of the solids.

4. Conclusion

A series of cationic polyurethanes (PUs) were synthesized by quaternizing different bromoalkane (C_2H_5Br, $C_8H_{17}Br$, and $C_{14}H_{29}Br$) with polyurethane, which were characterized by *in-situ* FTIR, NMR and GPC. Solid polymer electrolytes were prepared by complexes cationic PUs with different content of $LiClO_4$. All the solid polymer electrolytes had sufficient thermal stability as confirmed by TGA and exhibited a single-phase behavior evidenced by DSC results. For these electrolytes, FTIR spectra indicated the formation of polymer–ion complexes, in which the cation (Li^+) acts favoring the hard-soft segments miscibility. The ac impedance spectra show that the conductivity of the electrolytes follow the Arrhenius behavior, and ionic conductivity is associated with both the charge migration of ions between coordination sites and transmission of ions between aggregates, as confirmed by FT-IR and SEM. Alkyl quaternary ammonium salts in the polymer backbone

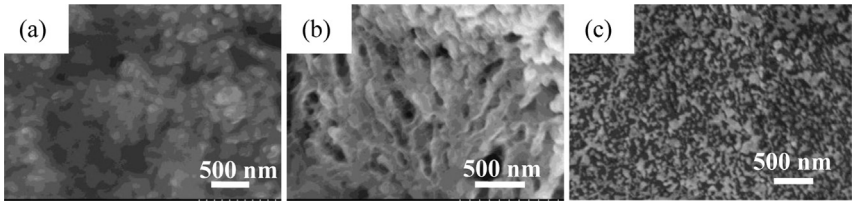

Fig. 6. SEM photographs of surface of PU-C_2 (a), PU-C_8 (b), and PU-C_{14} (c) with 30 wt% $LiClO_4$ content.

are recognized as inherent plasticizers, which make the electrolytes exhibit liquid-like behavior. The plasticizing effect of PU-C_8 and PU-C_{14} electrolytes are more effective than that of PU-C_2 electrolyte. Maximum ionic conductivity at room temperature for PU-C_8 electrolytes containing 50 wt% $LiClO_4$ reached 1.1×10^{-4} S cm^{-1}. The results presented herein, provide a new research idea that alkyl quaternary ammonium salts could be used as inherent plasticizers and facilitate ions transport. Useful insights into the various aspects of the electrochemical behavior of these systems and their dependence on the physico-chemical properties are needed to be studied further.

Acknowledgments

The financial supported by Program for Scientific Research Innovation Team in Colleges and Universities of Shandong Province, the National Natural Science Foundation of China (21204044, 21176147 and 21276149), Shandong Outstanding Young Scientist Award Fund (BS2012CL028) and Ji'nan Overseas Students Pioneer Plan (20120202) are gratefully acknowledged.

Appendix A. Supplementary data

Supplementary data related to this article can be found at http://dx.doi.org/10.1016/j.jpowsour.2013.10.116.

References

[1] H.P. Zhang, P. Zhang, Z.H. Li, M. Sun, Y.P. Wu, H.Q. Wu, Electrochem. Commun. 9 (2007) 1700–1703.
[2] F.M. Gray, Polymer Electrolytes; RSC Materials Monographs, The Royal Society of Chemistry, Cambridge, 1997.
[3] W.H. Meyer, Adv. Mater. 10 (1998) 439–448.
[4] N. Wu, Q. Cao, X. Wang, S. Li, X. Li, H. Deng, J. Power Sources 196 (2011) 9751–9756.
[5] R.L. Lavall, S. Ferrari, C. Tomasi, M. Marzantowicz, E. Quartarone, A. Magistris, P. Mustarelli, S. Lazzaroni, M. Fagnoni, J. Power Sources 195 (2010) 5761–5767.
[6] P. Santhosh, T. Vasudevan, A. Gopalan, K.P. Lee, J. Power Sources 160 (2006) 609–620.
[7] D. Saikia, Y.-H. Chen, Y.-C. Pan, J. Fang, L.-D. Tsai, G.T.K. Fey, H.-M. Kao, J. Mater. Chem. 21 (2011) 10542–10551.
[8] Y.-C. Yen, C.-C. Cheng, S.-W. Kuo, F.-C. Chang, Macromolecules 43 (2010) 2634–2637.
[9] C.A. Furtado, G. Goulart Silva, J.C. Machado, M.A. Pimenta, R.A. Silva, J. Phys. Chem. B 103 (1999) 7102–7110.
[10] T.-C. Wen, W.-C. Chen, J. Power Sources 92 (2001) 139–148.
[11] H.-H. Kuo, W.-C. Chen, T.-C. Wen, A. Gopalan, J. Power Sources 110 (2002) 27–33.
[12] N. Yoshimoto, H. Nomura, T. Shirai, M. Ishikawa, M. Morita, Electrochim. Acta 50 (2004) 275–279.
[13] J. Wang, W. Yang, J. Lei, J. Electrostat. 66 (2008) 627–629.
[14] S.K. Fullerton-Shirey, J.K. Maranas, Macromolecules 42 (2009) 2142–2156.
[15] S. Kohjiya, T. Kawabata, K. Maeda, S. Yamashita, Y. Shibata, in: B. Scrosati (Ed.), Second International Symposium on Polymer Electrolytes, Elsevier, London, 1990.
[16] Y. Ikeda, Y. Wada, Y. Matoba, S. Murakami, S. Kohjiya, Electrochim. Acta 45 (2000) 1167–1174.
[17] C. Robitaille, J. Prud'homme, Macromolecules 16 (1983) 665–671.
[18] N. Kobayashi, M. Uchiyama, K. Shigehara, E. Tsuchida, J. Phys. Chem. 89 (1985) 987–991.
[19] A. Killis, J.F. LeNest, A. Gandini, H. Cheradame, J.P. Cohen-Addad, Solid State Ionics 14 (1984) 231–237.
[20] M. Watanabe, S. Oohashi, K. Sanui, N. Ogata, T. Kobayshi, Z. Ohataki, Macromolecules 18 (1985) 1945–1950.
[21] H. Xia, M. Song, Soft Matter 1 (2005) 386–394.
[22] J. Wang, Z. Ye, H. Joly, Macromolecules 40 (2007) 6150–6163.
[23] L.F. Wang, Q. Ji, T.E. Glass, T.C. Ward, J.E. McGrath, M. Muggli, G. Burns, U. Sorathia, Polymer 41 (2000) 5083–5093.
[24] M. Ciosek, L. Sannier, M. Siekierski, D. Golodnitsky, E. Peled, B. Scrosati, S. Głowinkowski, W. Wieczorek, Electrochim. Acta 53 (2007) 1409–1416.
[25] H.S. Lee, Y.K. Wang, S.L. Hsu, Macromolecules 20 (1987) 2089–2095.
[26] X. Lu, R.A. Weiss, Macromolecules 24 (1991) 4381–4385.
[27] T.-C. Wen, M.-S. Wu, C.-H. Yang, Macromolecules 32 (1999) 2712–2720.
[28] J.D. Van Heumen, J.R. Stevens, Macromolecules 28 (1995) 4268–4277.
[29] W. Wieczorek, D. Raducha, A. Zalewska, J.R. Stevens, J. Phys. Chem. B 103 (1998) 8725–8731.
[30] B.L. Papke, M.A. Ratner, D.F. Shriver, J. Phys. Chem. Sol. 42 (1981) 493–500.
[31] P. Jannasch, Electrochim. Acta 46 (2001) 1641–1649.
[32] S.T.C. Ng, M. Forsyth, D.R. MacFarland, M. Garcia, M.E. Smith, J.H. Strange, Polymer 39 (1998) 6261–6268.
[33] J.R. MacCallum, C.A. Vincent, Polymer Electrolyte Reviews 1 and 2, Elsevier, London, 1987 and 1989.
[34] N. Wu, Q. Cao, X. Wang, X. Li, H. Deng, J. Power Sources 196 (2011) 8638–8643.
[35] G.G. Cameron, M.D. Ingram, in: J.R. MacCallum, C.A. Vincent (Eds.), Polymer Electrolyte Reviews, vol. 2, Elsevier, New York/London, 1989.
[36] J.M.G. Cowie, G.H. Spence, Polymer 39 (1998) 7139–7141.
[37] M. Clericuzio, W.O. Parker Jr., M. Soprani, M. Andrei, Solid State Ionics 82 (1995) 179–192.
[38] Y.-T. Kim, E.S. Smotkin, Solid State Ionics 149 (2002) 29–37.
[39] Y. Kato, K. Hasumi, S. Yokoyama, T. Yabe, H. Ikuta, Y. Uchimoto, M. Wakihara, Solid State Ionics 150 (2002) 355–361.